Applied Catalysis B: Environmental 140–141 (2013) 265–275

Contents lists available at SciVerse ScienceDirect

Applied Catalysis B: Environmental

journal homepage: www.elsevier.com/locate/apcatb

Isocyanate formation and reactivity on a Ba-based LNT catalyst studied by DRIFTS

Yaying Ji[a], Todd. J. Toops[b], Mark Crocker[a,*]

[a] Center for Applied Energy Research, University of Kentucky, Lexington, KY 40511, USA
[b] Fuels, Engines, and Emissions Research Center, Oak Ridge National Laboratory, Knoxville, TN 37932, USA

ARTICLE INFO

Article history:
Received 1 February 2013
Received in revised form 5 April 2013
Accepted 6 April 2013
Available online 15 April 2013

Keywords:
NOx reduction
Isocyanate
Ba nitrate
Carbon monoxide
Hydrolysis
Isotopic labeling

ABSTRACT

Diffuse reflectance infrared Fourier transform spectroscopy (DRIFTS) and mass spectrometry (MS), coupled with the use of isotopically-labeled reactants ($^{15}N^{18}O$ and ^{13}CO), were employed to study the formation of isocyanate species during NOx reduction with CO, as well as isocyanate reactivity toward typical exhaust gas components. DRIFTS demonstrated that both Ba–NCO and Al–NCO were simultaneously formed during NOx reduction by CO under dry lean-rich cycling conditions. The Ba–NCO band was more intense than that of Al–NCO, and became comparatively stronger at high temperatures. During rich purging at 300 and 400 °C, a near linear relationship was found between the increase in Ba–NCO band intensity and the decrease in Ba–NO_3 band intensity, suggesting that Ba–NCO is directly derived from the reaction of Ba nitrate with CO. Both temperature-programmed surface reaction (TPSR) and isothermal reaction modes (ISR) were utilized to study the reactivity of isocyanate species under lean conditions. Simultaneous DRIFTS and mass spectrometric measurements during TPSR indicated that isocyanate reaction with H_2O, O_2, NO and NO/O_2 took place almost immediately the temperature was raised above 100 °C, and that all NCO species were removed below 300 °C. The evolution of the NCO IR bands during ISR at 350 °C demonstrated that the kinetics of NCO hydrolysis are fast, although a delay in N_2 formation indicated that N_2 is not the initial product of the reaction. In contrast, immediate N_2 evolution was observed during NCO reaction with O_2 and with $NO + O_2$. Overall, it can be inferred that under dry cycling conditions with CO as the sole reductant, N_2 is mainly generated via NCO reaction with NO/O_2 after the switch to lean conditions, rather than being evolved during the rich phase. However, in the presence of water, isocyanate undergoes rapid hydrolysis in the rich phase, N_2 generation proceeding via NH_3.

1. Introduction

Lean NOx traps (LNTs), also referred to as NOx storage-reduction (NSR) catalysts, represent a promising technology for the abatement of NOx emissions from diesel and lean-burn gasoline engines. This technology requires cyclic operation between lean and rich conditions, corresponding to two different reaction phases. Under lean conditions, NO is oxidized to NO_2 and then stored in the form of nitrate (and/or nitrite). Upon periodic short excursions to rich conditions, stored NOx is released and reduced to N_2. To achieve these dual functions, LNT catalysts are typically composed of precious metals (generally Pt/Pd/Rh) and an alkali or alkaline-earth metal NOx storage component (most commonly BaO) supported on a high surface area metal oxide such as Al_2O_3 [1–3]. Although LNT technology has been commercialized for lean-burn gasoline and light-duty diesel applications, certain aspects of the mechanism of NOx storage and reduction are not fully understood. Relative to the NOx storage phase, understanding the chemistry of NOx reduction is particularly challenging. NOx reduction is generally performed over a very short period (usually 3–5 s), which creates difficulties in analyzing the chemistry of NOx reduction using standard laboratory techniques. Moreover, the involvement of different reducing agents (H_2, CO and hydrocarbons) in the NOx reduction process increases the complexity of NOx reduction chemistry. In an attempt to obtain insights into the NOx reduction process during rich purging, the NOx reduction system has been simplified in many studies by the use of H_2 as the sole reductant [4–9]. It has been generally proposed that reduction of stored NOx occurs via dissociative adsorption of released NOx and of hydrogen at Pt sites to form Pt–N, Pt–O, and Pt–H species, followed by recombination of surface Pt–N species to give dinitrogen and recombination of surface Pt–N and Pt–H species to give ammonia. Subsequent oxidation of ammonia with stored NOx and/or oxygen can generate additional N_2 [7–12].

Compared to H_2, CO has been shown to be a less effective reductant, especially at low temperature [13–18], albeit that Cant et al. reported that CO was more effective than H_2 during NOx

* Corresponding author. Tel.: +1 859 257 0295.
E-mail address: mark.crocker@uky.edu (M. Crocker).

0926-3373/$ – see front matter © 2013 Elsevier B.V. All rights reserved.
http://dx.doi.org/10.1016/j.apcatb.2013.04.017

reduction under dry conditions over a Pt-free catalyst [19]. It is generally believed that the poor NOx reduction behavior obtained with CO is due to Pt poisoning by CO at low temperature [20,21]. In general, the chemistry of NOx reduction by CO has drawn less attention than NOx reduction with H_2. Forzatti and co-workers investigated NOx reduction with CO under dry conditions by means of transient response methods [22–25]. They suggested that stored NOx was reduced by CO through a Pt-catalyzed surface pathway, in which nitrate was first reduced to nitrites and then surface isocyanate/cyanate species, followed by the reaction of these species with residual nitrates and nitrites to give dinitrogen. These studies also showed that isocyanate (–NCO) can be re-oxidized to surface nitrite and then nitrate upon exposure to oxygen, and that N_2 can be produced during the reduction of stored NOx by CO under rich purging and also during oxidation of surface NCO species by O_2 and NO/NO_2 during lean operation. However, under wet conditions, almost no NCO species were detected on the catalyst surface during NOx reduction with CO [22,26], this being ascribed to the hydrolysis of isocyanate to give ammonia [16,22,27,28]. Besides observing the hydrolysis of NCO species, Lesage et al. compared the reactivity of isocyanate with O_2 and with NO [28] and noted a lower reactivity of NCO toward NO compared to O_2. The results of these various studies suggest that isocyanate is an important intermediate during NOx reduction with CO. Moreover, recent research by DiGiulio et al. has demonstrated that the reactions of NCO with NO and O_2 are metal-catalyzed pathways, while the reaction of NCO with H_2O to produce NH_3 is not. They also emphasized that N_2 production via NCO can be significant [29]. However, a complete picture regarding the reactivity and role of isocyanate species in LNT catalysis is still lacking. Consequently, we undertook the current study in which DRIFTS was employed to monitor the evolution of surface species, while mass spectrometry was used to detect gaseous species formed during the reactions of surface NCO species. To aid in the differentiation of gaseous species in the mass spectrometer, isotopically-labeled reactants ($^{15}N^{18}O$ and ^{13}CO) were employed.

2. Experimental

2.1. Catalyst preparation

The preparation of $Pt/BaO/Al_2O_3$ has been described elsewhere [30]. Briefly, γ-alumina (Sasol, surface area of 132 m^2/g) was impregnated with aqueous $Ba(NO_3)_2$, dried and calcined at 500 °C in air. The Ba-loaded Al_2O_3 was subsequently impregnated with aqueous tetraammineplatinum(II) nitrate and further calcined at 500 °C. The Pt and BaO contents of the catalyst were 1 wt% and 20 wt%, respectively (the balance being Al_2O_3). Relative to the bare support, the catalyst shows decreased BET surface area and pore volume (98 m^2/g vs. 132 m^2/g and 0.32 cm^3/g vs. 0.43 cm^3/g). This decrease is mainly ascribed to the blocking of some pores during the loading of BaO on the support.

2.2. DRIFTS measurements

DRIFTS measurements were performed in an integrated stainless steel reaction cell, using a MIDAC model M2500 FTIR spectrometer coupled with a Harrick Scientific barrel ellipsoidal mirror DRIFT accessory. This specially designed DRIFTS assembly utilizes a barrel-shaped mirror that encompasses the catalyst sample. With the sample at one focal point of the ellipsoid and the detector at the opposite focal point, the system collects roughly 300° of the reflected IR signal and thus provides high sensitivity and high signal to noise ratios. The system is typically operated at slightly below atmospheric pressure (around 500 Torr) to prevent stagnation in the cell and to maintain the seal between the removable hemispherical ZnSe dome and the cell body. Mass flow controllers were used to establish the inlet gas concentrations, in conjunction with a sparger system submerged in a recirculating constant temperature bath that controlled the inlet concentration of H_2O. To minimize the initial spectral features associated with carbonates and achieve a good background spectrum, the catalyst was first pretreated under lean-rich cycling conditions at 300 °C overnight, followed by heating to 500 °C in H_2 to completely remove nitrate and carbonate. Clean initial background spectra were recorded every 50 °C in a decreasing sequence from 450 to 100 °C. The cycling gas composition for this initial pretreatment consisted of lean (300 ppm NO and 8% O_2 in Ar) and rich (1% H_2 in Ar) feeds.

Isocyanate formation was investigated in two different types of experiments involving cycling and continuous flowing conditions. For the lean-rich cycling study, the sample was repeatedly exposed to lean and rich phases until a "steady-state" cyclic condition was reached. This state is achieved when the final spectrum recorded at the end of the lean phase is identical to the final lean spectrum of the preceding cycle; additionally, the corresponding final rich phase spectra should also match for each cycle. A new spectrum was recorded every 5 s using an average of 8 scans (scan rate = 2 scans/s). The gas concentrations and times for each phase were: lean – 300 ppm NO, 8% O_2 in Ar for 6.5 min, and rich – 1% CO in Ar for either 2 or 1 min. For the study using continuous flowing gas, NOx was first stored at 300 °C using feed gas containing 300 ppm NO and 8% O_2 balanced with Ar for different periods of time, after which the sample was purged with Ar and cooled to 250 °C for NOx reduction by CO with two different concentrations: 1% CO and 0.35% CO. To maximize NCO formation, H_2O was not included in the feed (unless otherwise indicated). To study reactivity of NCO toward H_2O, a sparger system submerged in a recirculating constant temperature bath was used to deliver the desired concentration of water vapor in an Ar flow.

Isocyanate reactivity was tested by two different methods: temperature-programmed surface reaction (TPSR) and isothermal surface reaction (ISR). For the TPSR study, isocyanate species were first generated on the catalyst surface at 350 °C by reaction of NO with CO (500 ppm NO and 1% CO in Ar). Different from the standard approach of generating isocyanate by reduction of stored NOx with CO, use of the NO + CO reaction can generate significant amounts of isocyanate on the catalyst surface but with very limited formation of nitrate; this avoids excessive interference from nitrate bands during the study of NCO reactivity. This approach has been reported by Bion et al. [31]. In order to differentiate N_2 from CO in the mass spectrometer, labeled $^{15}N^{18}O$ and ^{13}CO were used in these experiments. After the surface was saturated by NCO species at 350 °C, followed by cooling to 100 °C in flowing NO + CO, DRIFTS scans were recorded every 10 s using 10 averaged scans at 100 °C, after which the gas was switched to the desired gas for the TPSR experiment. The TPSR study was performed at intervals of 50 °C from 100 °C to 450 °C, using a heating rate of 5 °C/min between each dwell temperature. At each temperature, spectra were recorded using 100 averaged scans. Different from TPSR, ISR experiments were used to investigate the qualitative kinetics of NCO reactions. NCO species were first generated on the catalyst surface by reaction of NO with CO at 350 °C for 5 min, after which the feed gas was switched to one containing the desired reactant. During reaction, spectra were recorded every 10 s using a 10 scan average. The NCO reaction conditions consisted of one of the following: (i) Ar, (ii) 0.6% O_2, (iii) 500 ppm NO, (iv) 500 ppm NO + 0.6% O_2, or (v) 3.5% H_2O. In all cases Ar was used as the balance gas.

2.3. Mass spectrometry

A mass spectrometer (Stanford Research Systems RGA100 with electron multiplier) was used to detect the evolution of gaseous

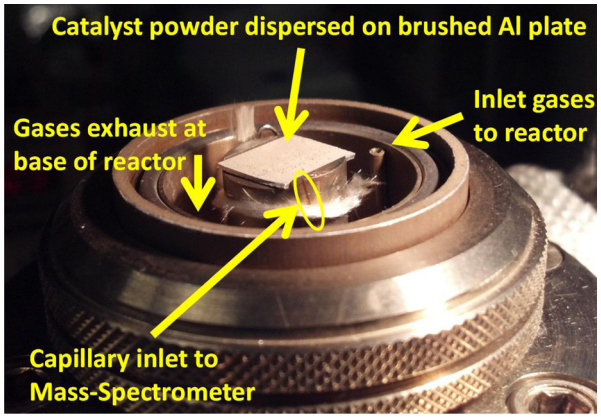

Fig. 1. Photograph of reactor used for DRIFTS-MS measurements. Infrared-transparent dome made of ZnSe sits on top of reactor to enable environmental control and IR access.

species during NCO reaction. As shown in Fig. 1, a capillary with an i.d. of 76 μm and o.d. of 197 μm (polyamide coating thickness of 13.5 μm) was inserted into the DRIFTS cell to sample the gaseous species formed. The masses that were monitored consisted of: 29 (^{13}CO), 30 ($^{15}N^{15}N$), 31($^{15}N^{16}O$), 32 ($^{16}O^{16}O$), 45 ($^{13}C^{16}O^{16}O$), 46 ($^{15}N^{15}N^{16}O$), 47 ($^{13}C^{16}O^{18}O$ and $^{15}N^{16}O^{16}O$), 48 ($^{15}N^{15}N^{18}O$), 49 ($^{15}N^{16}O^{18}O$ and $^{13}C^{18}O^{18}O$), and 51 ($^{15}N^{18}O^{18}O$). To achieve real time resolution and alignment with DRIFTS data during NCO reaction, Kr ($m/e = 84$) was included in the experiments as a reference.

3. Results

3.1. Isocyanate formation under cycling conditions

Under cycling conditions at 200 °C, almost no isocyanate species were detected by DRIFTS due to the poor NOx reduction efficiency by CO at this relatively low temperature. Consequently, experiments were focused on NOx reduction behavior at 300 °C and 400 °C after NOx was stored as Ba nitrate during lean operation. Fig. 2 shows DRIFTS data obtained during rich purging with CO as reductant under "steady-state" cycling conditions (300 ppm NO + 8% O_2 for 6.5 min and 1% CO in Ar for 2 min) in the absence of H_2O in order to maximize NCO formation during rich purging. At 300 °C (Fig. 2a), significant gaseous CO_2 (2313/2325 cm^{-1}) is first observed after switching to rich conditions, after which both Pt–CO (2072 cm^{-1}) and NCO bands around 2200 cm^{-1} appear simultaneously. These observations can be understood on the basis that Pt is present in an oxidized state (PtO_x) during lean phase operation. After switching to rich conditions PtO_x needs to be first reduced to metallic Pt before significant CO adsorption can occur, as evidenced by CO_2 evolution at the beginning of rich purging. With increasing time during NOx reduction with CO, two discrete isocyanate bands become visible. Based on the literature [16,26,27,29], these bands can be assigned as Ba–NCO (2160 cm^{-1}) and Al–NCO (2220 cm^{-1}), although it should be noted that Forzatti et al. [23] have suggested that the bands are related to isocyanate/cyanate species on the Ba phase. Both bands continuously grow with time during rich purging, although the Ba–NCO band possesses a faster growth rate than the (presumed) Al–NCO band, such that a Ba–NCO/Al–NCO band intensity ratio of 1.9 is obtained at the end of rich purging (i.e., after 2 min). In contrast to NOx reduction behavior at 300 °C, a Pt–CO band is not observed at 400 °C during NOx reduction with CO (Fig. 2b). Similar to the observations made at 300 °C, both isocyanate bands grow with time although the final ratio of Ba–NCO/Al–NCO band intensities is 3.0, implying that more Ba–NCO is formed at 400 °C than at 300 °C relative to Al–NCO. This suggests either that Al–NCO possesses lower thermal stability than Ba–NCO or that transformation of Al–NCO to Ba–NCO takes place at 400 °C. In addition, a continuous decrease of Ba-nitrate band intensity (1320 and 1410 cm^{-1}) with time is observed during rich purging at both temperatures.

To gain additional insights, a series of difference spectra was obtained by subtracting rich phase spectra at different stages of NOx reduction with CO from the spectra collected at the end of the lean phase. As shown in Fig. 3, a negative carbonate peak at 1560 cm^{-1} was observed at both temperatures under rich conditions, indicative of carbonate formation during rich purging; this has been observed previously [23,26]. Reduction of Ba nitrate proceeded during the entirety of the rich phase (2 min) at 300 °C, as evidenced by a continuous decrease in Ba nitrate band intensity with time (corresponding to an increase in the intensity of the 1320 cm^{-1} band in the difference spectra). No nitrite species were observed during reduction. At 400 °C, there was no noticeable change in Ba nitrate band intensity after 95 s, i.e., Ba nitrate reduction mainly occurred in the first 95 s during rich purging with CO, implying that a shorter rich period of time was required to reduce Ba nitrate at 400 °C than at 300 °C. The time dependence of Ba–NCO formation and of Ba nitrate reduction (as reflected in the band intensities in difference spectra) is plotted in Fig. 4a. An induction period for both Ba–NCO formation and Ba nitrate reduction is observed at the beginning of the rich phase, corresponding to 30 s at 300 °C and 20 s at 400 °C, respectively. As noted above, this delay can be ascribed to the reduction of oxidized Pt. The shorter induction period at 400 °C relative to 300 °C is presumably a consequence of the Pt reduction kinetics being faster at 400 °C. Significant Ba–NCO formation was observed during the first 40 s after the

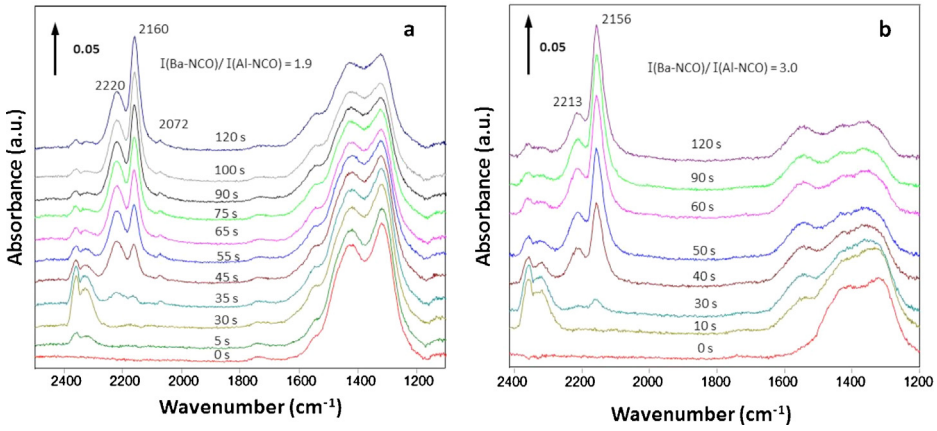

Fig. 2. Evolution of isocyanate bands during rich purging under cycling conditions: (a) 300 °C and (b) 400 °C.

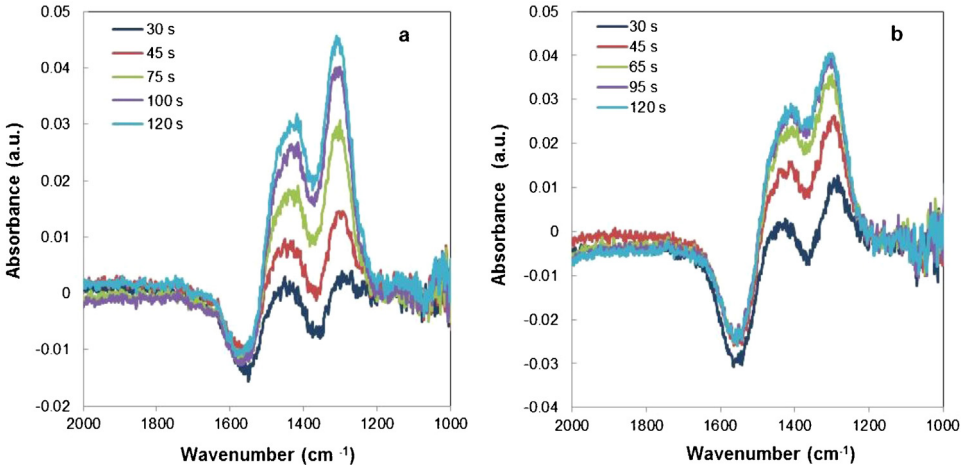

Fig. 3. Difference spectra obtained by subtraction of rich phase spectra from lean phase spectra acquired under cycling conditions: (a) 300 °C and (b) 400 °C. Note that the duration of the rich phase was 120 s.

induction period, after which the Ba–NCO band grew more slowly. In contrast, the Ba–NCO band grew more slowly and constantly during the entire NOx reduction period (2 min) at 300 °C. Meanwhile, a similar trend was found for the reduction of Ba nitrate, the kinetics of NOx reduction with CO being clearly faster at 400 °C than at 300 °C.

Fig. 4b displays the correlation of Ba–NCO formation (increase in intensity of 2160 cm^{-1} band) with Ba-nitrate reduction (decrease in 1320 cm^{-1} band intensity). It is interesting to see that an almost linear relationship exists at both 300 °C and 400 °C, although the two plots have slightly different slopes. The fact that a straight line is obtained indicates that δ[nitrate]/δ[NCO] is constant. Assuming that isocyanate does not react further at a significant rate, this implies that a certain fraction of the nitrate groups react to form isocyanate, this fraction being different at the two temperatures studied. The assumption that isocyanate is stable under these conditions (i.e., in the presence of the CO feed) and for the short duration of the experiment (2 min), is confirmed by DRIFTS data which show that Ba–NCO removal is slow (see Section 3.2). A smaller slope of 0.35 was obtained at 400 °C relative to the slope of 0.40 at 300 °C, implying that more Ba–NCO species can be generated at 400 °C with the same amount of Ba nitrate being reduced, i.e., Ba–NCO formation is more efficient at 400 °C relative to 300 °C. Overall, the linear correlation between Ba–NCO formation and Ba-nitrate reduction infers a close relationship between these two events, and based on the reactivity of NCO species (vide infra), leads to the conclusion that Ba–NCO species represent a critical intermediate in the reduction of NOx with CO. In the case of Al–NCO, a much slower increase in intensity with time was observed during rich purging, consistent with the comparatively lower final Al–NCO band intensity.

3.2. Isocyanate formation under continuous flowing conditions

Isocyanate formation was further investigated under continuous flowing conditions. NOx was first stored on the catalyst by flowing NO/O_2 at 300 °C for different periods of time. After purging with Ar and cooling to 250 °C, the feed gas was switched to CO for NOx reduction. Fig. 5 displays the Ba–NCO band intensity as a function of time. For the same amount of NOx stored (corresponding to a storage time of 0.5 h), the concentration of CO has a relatively small impact on Ba–NCO formation. Specifically, increasing the CO concentration from 0.35% to 1% results in only a slight increase in the Ba–NCO formation rate during the first 5 min of NOx reduction. Compared to the use of 0.35% CO, NOx reduction with 1% CO affords a higher maximum Ba–NCO band intensity during extended NOx reduction. In both cases, after reaching its maximum, the Ba–NCO band undergoes a very gradual decrease in intensity, suggesting that isocyanate removal is slow under these conditions. Notably, a continuous decrease in the intensity of the Ba nitrate bands was

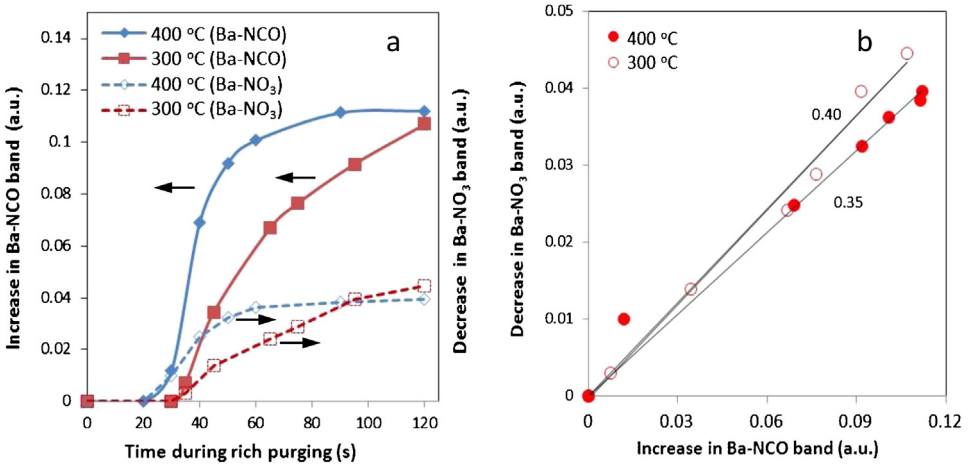

Fig. 4. (a) Time dependence of Ba–NCO and Ba–NO_3 signal intensities during rich purging under cycling conditions. (b) Correlation of increase in Ba–NCO signal intensity with decrease in Ba–NO_3 signal intensity under cycling conditions.

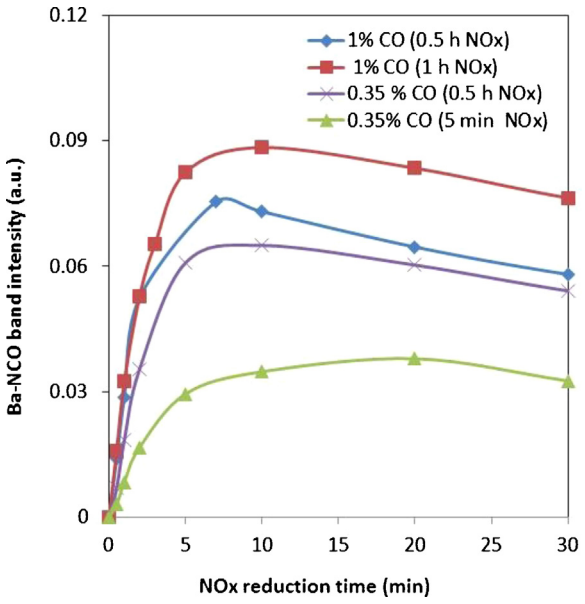

Fig. 5. Evolution of Ba–NCO band intensity during NOx reduction under continuous flowing conditions at 250 °C.

observed during reduction although the decrease became slower with time increasing. Moreover, a continuous increase in carbonate species was also observed. These results infer that a further, slow reaction between Ba–NCO and Ba–NO_3 species occurred during the later stages of reduction, this being consistent with reports by Forzatti et al. [23] and Di Giulio et al. [29]. For experiments in which a constant CO concentration of 1% CO was used, a similar Ba–NCO formation rate was observed during the first 2 min of NOx reduction for different NOx loadings (0.5 h vs. 1 h). However, the amount of NOx stored did affect the maximum Ba–NCO band intensity, as evidenced by an increased Ba–NCO maximum for the 1 h NOx storage time relative to the 0.5 h NOx storage time.

3.3. Isocyanate reactivity

3.3.1. Temperature-programmed surface reaction (TPSR)

Although isocyanate has been implicated as an important intermediate during NOx reduction by CO, the reactivity of isocyanate toward the various gas species present in lean exhaust gas has not been widely reported in the literature. In this study, a combined MS-DRIFTS technique was utilized to allow simultaneous detection of both surface and gas species. Labeled $^{15}N^{18}O$ and ^{13}CO were used to generate isocyanate species at 350 °C in order to enable mass spectrometry to distinguish between gaseous N_2 (m/e = 30 based on ^{15}N) and CO (m/e = 29 based on ^{13}C) during reaction. The evolution of surface species during TPSR under different atmospheres is illustrated in Fig. 6. Compared to unlabeled NO and CO, a red shift for both isocyanate bands was observed when feeding $^{15}N^{18}O$ and ^{13}CO, the wavenumber shifting from ~2220 cm^{-1} to 2160 cm^{-1} for Al–NCO and from 2160 cm^{-1} to 2080 cm^{-1} for Ba–NCO. Note that the magnitude of this shift (80 cm^{-1}) is consistent with the incorporation of ^{15}N and ^{13}C isotopes into the NCO group [32]. After NCO species were generated on the surface at 350 °C by reaction of NO and CO, followed by cooling to 100 °C, the gas atmosphere applied was switched from NO + CO to O_2 for temperature-programmed reaction. As shown in the inset of Fig. 6, an immediate decrease in band intensity was observed for the bands at 2160 cm^{-1} (Al–NCO) and 2031 cm^{-1} (Pt–CO) after the feed was switched from NO + CO to O_2 at 100 °C, indicating both removal of CO adsorbed on Pt sites by O_2 and a lower stability of Al–NCO species toward O_2 compared to Ba–NCO. Upon increasing the temperature, both Al–NCO and Ba–NCO bands exhibited a significant decline in intensity in the temperature range 200–300 °C, both isocyanate species having almost completely disappeared at ~300 °C. Simultaneously, growth of the Ba nitrate band and a decline in the carbonate band were observed with increasing temperature.

Table 1
Summary of the main mass contributions of different molecules of interest.

Mass number	Parent molecule	
	Expected	Possible
30	^{15}N–^{15}N	
31	^{15}N–^{16}O	^{13}C–^{18}O
33	^{15}N–^{18}O	
45	^{13}C–^{16}O–^{16}O	
46	^{15}N–^{15}N–^{16}O	
47	^{13}C–^{16}O–^{18}O	^{15}N–^{16}O–^{16}O
48	^{15}N–^{15}N–^{18}O	
49	^{15}N–^{16}O–^{18}O	^{13}C–^{18}O–^{18}O

In the case of isocyanate exposure to NO, only a slight drop in the intensity of the bands at 2160 cm^{-1} (Al–NCO) and 2031 cm^{-1} (Pt–CO) was observed during gas switching compared to the case of O_2. However, a significant drop in the intensity of both bands occurred at ~200 °C, and both isocyanate species completely disappeared at 250 °C, demonstrating the lower stability of both isocyanate species under NO compared to O_2. Additionally, during TPSR with NO, a Ba nitrite band (1167 cm^{-1}) was observed at 200 °C, indicative of NO storage. This band disappeared at 250 °C, while significant formation of Ba nitrate was also detected.

Compared to TPSR under O_2 and NO, the evolution of Al–NCO and Ba–NCO species under NO + O_2 showed different behavior. Evolution of the band intensity ratio between Al–NCO and Ba–NCO inferred that both O_2 and NO are involved in the reaction, while the overall reactivity was improved by co-feeding NO+O_2, as evidenced by the fact that almost no isocyanate species remained on the surface at 225 °C, this being lower than the temperature of 250 °C required in the NO case. Compared to TPSR under NO, significant formation of Ba nitrate was detected under NO + O_2 flow, which can be ascribed to the oxidation of nitrite by O_2 and to the formation of NO_2 due to oxidation of NO by O_2 with subsequent storage of NO_2 as nitrate.

In comparison to NO + O_2, water is significantly more reactive toward isocyanate. After switching from NO + CO to H_2O at 100 °C, the Al–NCO species (2160 cm^{-1}) almost completely disappeared, while the Ba–NCO species were almost unchanged. This finding demonstrates the different reactivity of Al–NCO and Ba–NCO toward H_2O, which is similar to TPSR under O_2. When the temperature was raised to 200 °C, almost all the isocyanate species were removed from the surface. Evidently, H_2O is extremely reactive toward isocyanate species as compared to the other species present in lean exhaust gas. Finally, the stability of isocyanate was investigated under flowing Ar. As displayed in Fig. 6, the evolution of the isocyanate bands indicated that Al–NCO was more reactive than Ba–NCO. With increase of the temperature, both isocyanate species were removed at ~300 °C. A slight decrease in the intensity of the nitrate band below 300 °C again implies the occurrence of a reaction with NCO species [23,29].

The evolution of gaseous species was monitored in the TPSR experiments by mass spectrometry. Evolution of the highlighted mass species (as listed in Table 1) during TPSR under different atmospheres is depicted in Fig. 7. During TPSR in O_2, a large amount of mass 45 ($^{13}C^{16}O_2$) was detected, the peak concentration being reached around 170 °C. Mass 30 ($^{15}N_2$) and mass 46 ($^{15}N_2{}^{16}O$) were also detected, and both showed similar trends with respect to temperature, inferring that both of them can be formed from the same reaction approach. No $^{15}N^{16}O$ (mass 31) or $^{15}N^{18}O$ (mass 33) were detected during the TPSR. Meanwhile, small amounts of mass 48

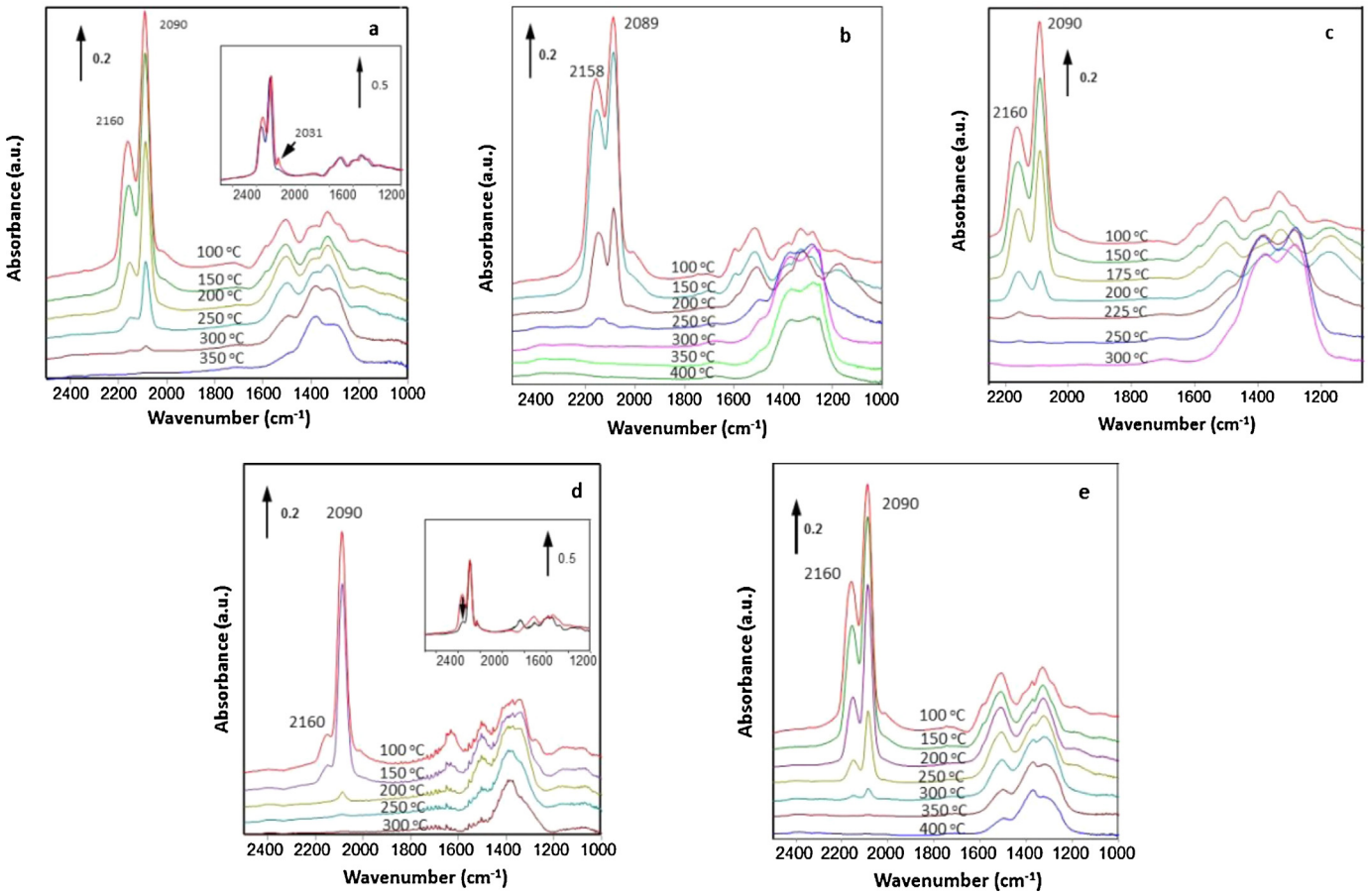

Fig. 6. Evolution of surface species during TPSR under different conditions: (a) O_2; (b) NO; (c) NO + O_2; (d) H_2O and (e) Ar. The insets in (a) and (d) show a comparison of spectra immediately before and after switching to O_2 and H_2O at 100 °C, respectively.

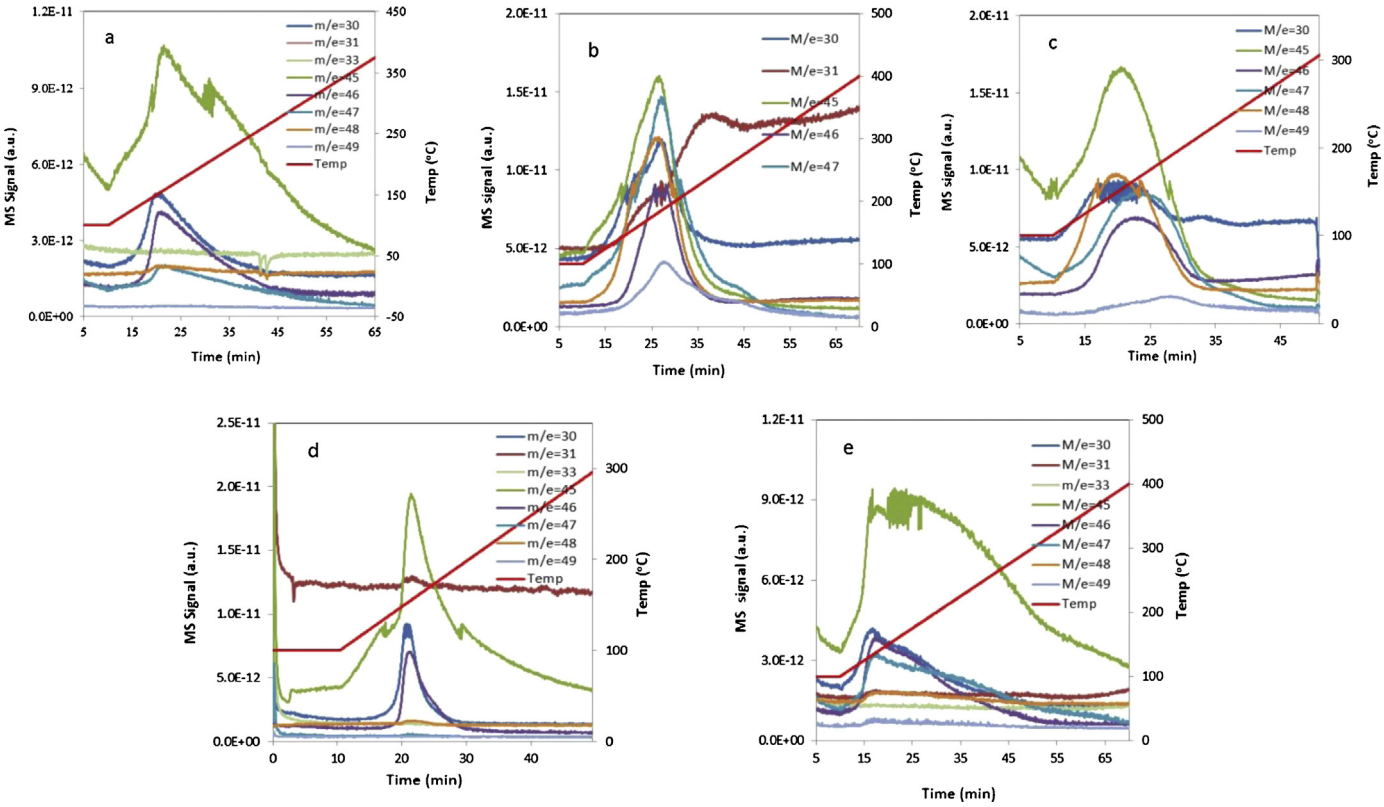

Fig. 7. Evolution of MS signals during TPSR under different conditions: (a) O_2; (b) NO; (c) NO + O_2; (d) H_2O and (e) Ar.

($^{15}N_2{}^{18}O$) and mass 47 were observed during the TPSR experiment. As shown in Table 1, two different molecules, $^{13}C^{16}O^{18}O$ and $^{15}N^{16}O^{16}O$, can contribute to mass 47. According to the generally accepted mechanism for NCO formation, the O in NCO should be ^{16}O, which originates from $^{13}C^{16}O$. During O_2-TPSR, the O_2 contained only ^{16}O atoms, and so mass 47 most likely corresponded to $^{15}N^{16}O^{16}O$. The formation of these N-containing species was observed in the temperature range 100–250 °C. Combining this information with the DRIFTS data for the TPSR experiments, it is apparent that these gaseous species were mainly generated from the decomposition of Al–NCO and Ba–NCO species via reaction with O_2. Subsequently, the NO_2 that was detected formed nitrates, as previously shown in Fig. 6.

Compared to O_2-TPSR, reaction under NO shows different features. Detection of $^{13}C^{16}O_2$ (mass 45) commenced immediately upon heating above 100 °C, two different evolution maxima at 140 °C and ~170 °C being apparent. Mass 30 ($^{15}N_2$), mass 46 ($^{15}N_2{}^{16}O$), mass 47, mass 48 ($^{15}N_2{}^{18}O$) and mass 49 were also observed with the same evolution trend as mass 45. It is also noteworthy that two different types of N_2O, being related to two different O atoms (^{16}O and ^{18}O), are observed during this reaction. Given that the O atom in NCO derives from $^{13}C^{16}O$, mass 47 and mass 49 in this case are related to $^{13}C^{16}O^{18}O$ (not $^{15}N^{16}O^{16}O$) and $^{15}N^{16}O^{18}O$, respectively. The trend for $^{15}N^{18}O$ (mass 33) shows an obvious consumption peak at around 170 °C, which is in line with the release event. Relative to O_2-TPSR, N_2 (mass 30), N_2O (mass 46 and mass 48) and NO_2 (mass 49) release peaks are more intense, being situated in a narrower temperature window.

Turning to TPSR under NO + O_2, relatively more CO_2 and less N_2, N_2O and NO_2 were detected compared to NO-TPSR, implying that the presence of O_2 impaired selective oxidation of NCO to N_2, with relatively more NCO being oxidized to NO or NO_2 (which was stored at nitrate). In addition, all of the gaseous species detected during reaction in NO + O_2 possessed slightly lower release temperatures (~150 °C) relative to the case of NO (~170 °C), which is consistent with the evolution of NCO species as observed by DRIFTS.

In the case of TPSR with H_2O, a sharp peak for $^{13}C^{16}O_2$ (mass 45) evolution was immediately detected after switching to H_2O at 100 °C. Correlating this observation with the DRIFTS data, this fraction of $^{13}C^{16}O_2$ was mainly produced from the reaction of H_2O with Al–NCO. Additional formation of $^{13}C^{16}O_2$ (mass 45) was observed upon raising the temperature above 100 °C, its maximum being reached at 160 °C. $^{15}N_2$ (mass 30) and $^{15}N_2{}^{16}O$ (mass 46) were also observed in this experiment, their formation mainly being situated in the range 130–200 °C, a narrower range than in the case of NO and O_2 (i.e., from 100 to 250 °C), being in agreement with the evolution of NCO species. Compared to CO_2 formation, there was a slight delay in the formation of N_2, with a sharp N_2 formation peak being observed in this case. A very small $^{15}N^{16}O$ release peak was observed at ~160 °C, while almost no $^{15}N_2{}^{18}O$ (mass 48) was detected during this TPSR. Compared to TPSR under NO or O_2, lower formation of N_2, N_2O and NO_2 was found during TPSR under H_2O.

The reactivity of isocyanate under Ar (i.e., toward nitrate) was also studied by this temperature-programmed method. As shown in Fig. 7, evolution of $^{15}N_2$ (mass 30) started at ~100 °C and ended at ~300 °C, this temperature window being slightly extended compared to the other cases. Except for mass 47, the evolution of the other gaseous species was similar to that during O_2-TPSR.

A further comparison of $^{15}N_2$ evolution during TPSR is shown in Fig. 8. Similar to Ar-TPSR, evolution of N_2 during O_2-TPSR occurred in a very wide temperature range, the maximum being reached at 150 °C. In the case of TPSR with H_2O, the situation of N_2 formation was very different. N_2 generation commenced at a slightly higher temperature (~130 °C) although N_2 formation was observed across a very narrow temperature range. N_2 evolution during

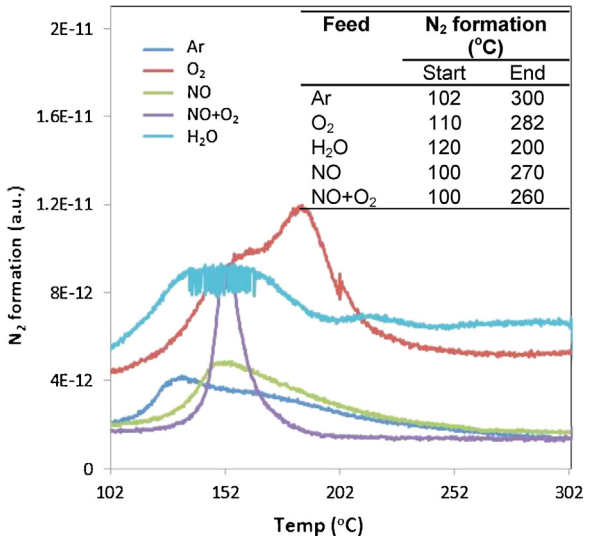

Fig. 8. Comparison of N_2 formation during NCO-TPSR under different conditions. *Note*: the oscillations in the trace for the H_2O experiment are an artifact produced by the mass spectrometer.

NO + O_2-TPSR occurred in a slightly lower temperature range relative to that in NO-TPSR. The most significant N_2 formation was found in NO-TPSR, while there was a decrease in N_2 formation during TPSR when co-feeding NO and O_2. In contrast, Ar- and H_2O-TPSR exhibited lower formation of N_2. A detailed comparison of $^{15}N_2$ formation during TPSR is shown in the inset of Fig. 8. In most cases, N_2 formation started almost immediately after the temperature was raised above 100 °C and ceased before 300 °C. In principle, this could occur via reaction with the feed gas, via reaction with nitrates or via Pt-catalyzed decomposition. However, the latter route can be excluded on the basis that CO was not evolved during TPSR under Ar. The fact that CO_2 was evolved (Fig. 7), indicates that NCO species underwent oxidation during Ar-TPSR, i.e., via reaction with nitrate groups.

3.3.2. Isothermal reaction (ISR)

To obtain insights into the reactivity of NCO at higher temperatures, an additional study was performed at 350 °C. NCO was first generated by reaction of NO and CO at 350 °C, followed by switching to the desired gas. The evolution of surface species during this isothermal reaction (ISR) is depicted in Fig. 9. In the case of ISR under O_2, a slightly faster decrease in Ba–NCO band intensity relative to Al–NCO infers that Ba–NCO species are more reactive toward O_2 than Al–NCO at this temperature. A growth in Ba nitrate bands was also observed during O_2-ISR. Similar to ISR under O_2, Ba–NCO species also displayed slightly higher reactivity than Al–NCO when exposed to NO, although Ba–NCO appeared less reactive toward NO than O_2 under these conditions as revealed by a slightly slower evolution of NCO under NO than under O_2. Although the nitrate bands became stronger with time, Ba nitrate generated during NO-ISR is less intense than that in O_2-ISR. In the case of ISR under NO + O_2, the evolution of the surface species was more similar to O_2-ISR than NO-ISR. Moreover, the observation that the Ba–NCO and Al–NCO bands disappeared at a slightly faster rate than under O_2, suggests the participation of NO_2 in NCO oxidation. This is consistent with the results of the corresponding TPSR experiments presented above.

Unlike the foregoing ISR experiments, introduction of H_2O resulted in a rapid removal of NCO species. Indeed, most of the NCO species were removed in the first 20 s, and NCO completely disappeared at around 30 s, demonstrating the high reactivity of both Al–NCO and Ba–NCO species toward H_2O (albeit that Al–NCO

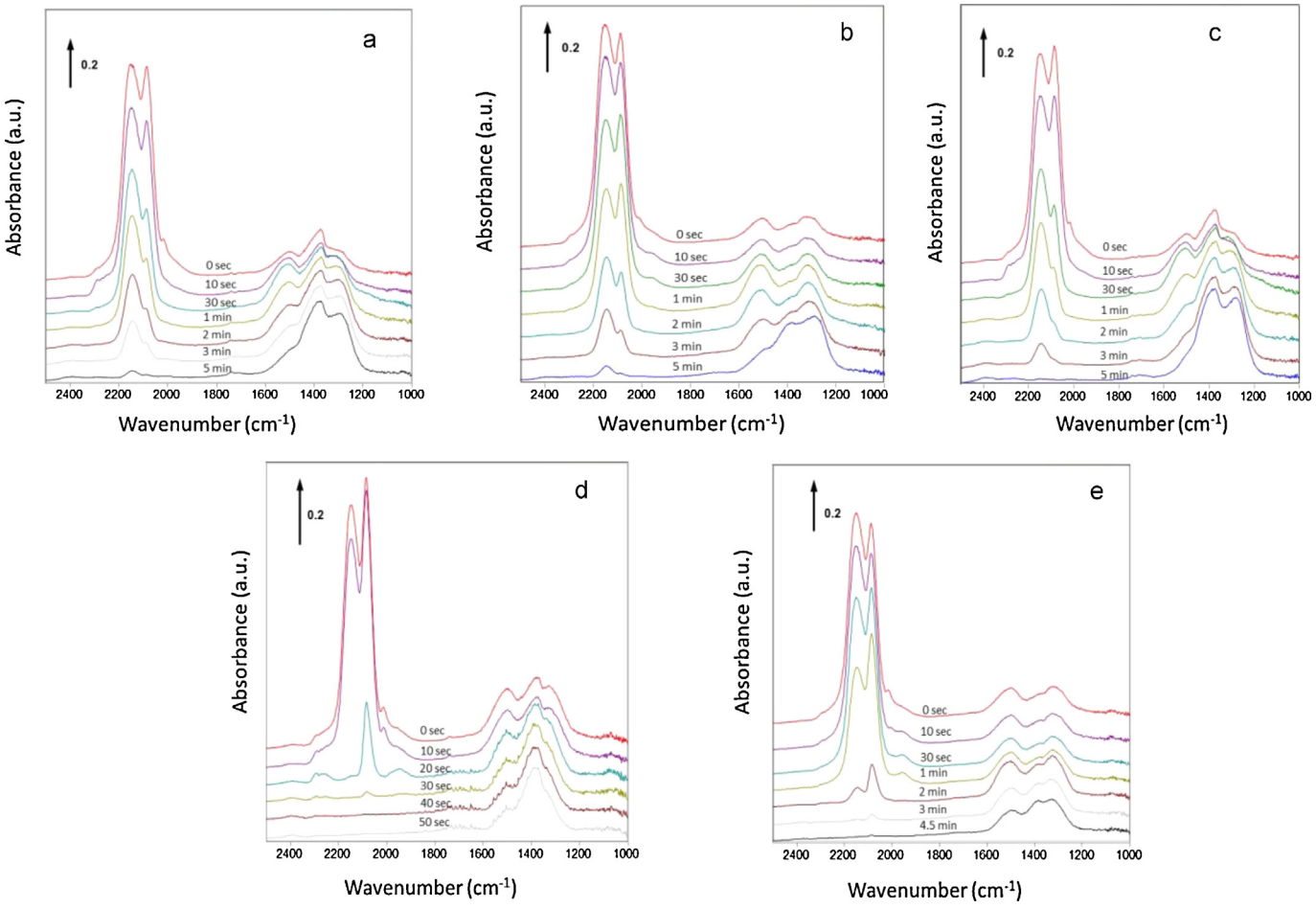

Fig. 9. Evolution of DRIFT spectra during isothermal reaction of isocyanate at 350 °C under different conditions: (a) O_2; (b) NO; (c) NO+O_2; (d) H_2O and (e) Ar.

was consumed before Ba–NCO). Therefore, it is not difficult to understand why almost no NCO species can be detected under typical lean-rich cycling conditions when H_2O is present. The stability of isocyanate species was also studied at 350 °C in Ar flow. A significant change in NCO band intensity was observed within 1 min. The faster removal of Al–NCO relative to Ba–NCO further demonstrates that Al–NCO species are more reactive than Ba–NCO.

The evolution of gaseous products during the ISR study was monitored by mass spectrometry. Fig. 10 compares the evolution of the N-containing species during reaction at 350 °C. For ISR under O_2, a rapid release of $^{15}N_2$ (mass 30), $^{15}N_2{}^{16}O$ (mass 46) and $^{15}N^{16}O^{18}O$ (mass 49) was observed after switching to O_2. N_2 release was observed over a short period (~1 min), while evolution of $^{15}N_2{}^{16}O$ (mass 46) extended up to 5 min. A small $^{15}N_2{}^{18}O$ (mass 48) peak was also observed. It can be concluded that not all the NCO species were oxidized to N_2, a significant fraction of the NCO species being oxidized to N_2O and NO_2. This is why the Ba nitrate IR bands became stronger during the reaction.

Unlike O_2-ISR, ISR under NO afforded N_2 as the only product (small peaks at masses 46, 48 and 49 being confirmed as impurities present in the NO feed). The broad nature of the N_2 peak indicated that N_2 formation occurred over a long period. The trends under NO + O_2 were again very similar to those observed for O_2, inferring that the reaction under NO + O_2 is dominated by O_2 rather than NO; this can be ascribed to the faster kinetics of NCO oxidation by O_2 and possibly NO_2 formed from NO oxidation than by NO (at the O_2 and NO concentrations used in this study).

In the case of isocyanate reaction with H_2O, a delay in N_2 (mass 30) formation was observed. NH_3 is also expected to be a product of NCO reaction with H_2O [16,23,27], but interference from water made this impossible to detect with the mass spectrometer used. Additionally, sharp release peaks for mass 46 and mass 49, corresponding to $^{15}N_2{}^{16}O$ and $^{15}N^{16}O^{18}O$, rapidly appeared after switching to H_2O. Notably, DRIFT spectra (Fig. 9d) show a decrease in the intensity of the 1320 cm^{-1} nitrate band after the switch, suggesting that some of the nitrate species were released (displaced by H_2O) as $^{15}N^{16}O^{18}O$. Note that the nitrates present are expected to contain both ^{18}O and ^{16}O, derived from the reaction of $^{15}N^{18}O$ with $Ba^{16}O$.

Finally, in the case of ISR under Ar, gas evolution tends to be simple relative to other cases. $^{15}N_2$ (mass 30) and $^{15}N_2{}^{16}O$ (mass 46) were two main gas species detected during this reaction. N_2 formation was observed after 2 min of reaction, consistent with a slow reaction of the isocyanate species with nitrate.

Evolution of $^{15}N_2$ (mass 30) during ISR under different atmospheres is further compared in Fig. 11. A spike of N_2 formation observed after switching to O_2 and NO/O_2 indicates the kinetics of the NCO reaction with O_2 are fast. In contrast, the kinetics of N_2 formation were relatively slower during isocyanate exposure to NO, consistent with results reported by Lesage et al. [27]. N_2 formation under Ar again indicated that NCO can undergo reaction with nitrate to release N_2, albeit that the reaction is relatively slow. Finally, for isocyanate reaction with H_2O, a 4 s delay was noted until the appearance of N_2, although the reaction was complete in only 0.7 min. Moreover, the amount of N_2 formed was

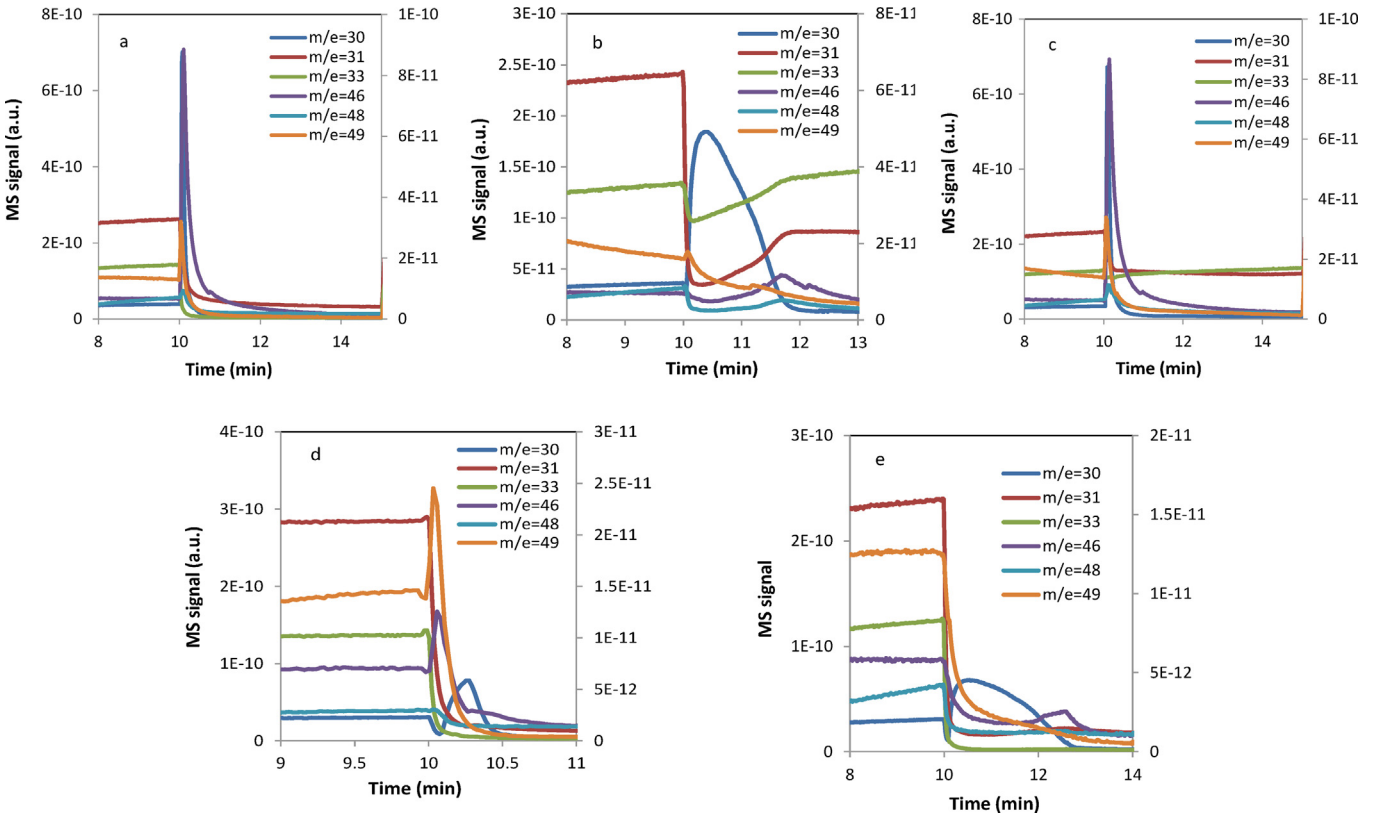

Fig. 10. Evolution of MS signals during isothermal reaction at 350 °C under different conditions: (a) O_2; (b) NO; (c) NO + O_2; (d) H_2O and (e) Ar. Signal intensities for masses 46, 48 and 49 correspond to the secondary *y*-axis.

small relative to the initial amount of NCO species present on the surface prior to reaction. This suggests that N_2 is not the initial reaction product, N_2 being produced through a secondary reaction of NH_3 (the direct product from NCO hydrolysis [16,23,27]), with residual NOx. By integration of the N_2 evolution profiles, the quantity of N_2 formed during these reactions can be compared. As shown in the insert of Fig. 11, the N_2 peak areas follow the order: NO > Ar > NO + O_2 > O_2 > H_2O.

4. Discussion

Two mechanisms for the reduction of stored NOx by CO under dry conditions over Pt/Ba/Al_2O_3 catalyst have been reported in the literature. The first one was discussed by Szailer et al. [16] and Schouten et al. [20], and involves several steps as shown below:

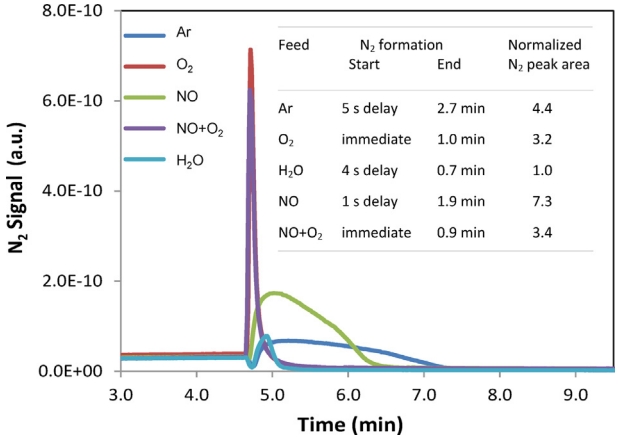

Fig. 11. Time dependence of N_2 formation during isothermal reactions of isocyanate at 350 °C.

$$(1+x)Pt* + NOx \rightarrow Pt{-}N + xPt{-}O \quad (1)$$

$$2Pt{-}N \rightarrow 2Pt* + N_2 \quad (2)$$

$$Pt{-}N + Pt{-}NO \rightarrow 2Pt* + N_2O \quad (3)$$

$$Pt* + CO \rightarrow Pt{-}CO \quad (4)$$

$$Pt{-}CO + Pt{-}N \rightarrow Pt{-}NCO + Pt* \quad (5)$$

$$Pt{-}NCO + Pt{-}NO \rightarrow 2Pt* + N_2 + CO_2 \quad (6)$$

In this mechanism, NOx stored on Ba sites has to first migrate to Pt sites. NOx species dissociated on Pt sites can either form N_2 or react with CO adsorbed on adjacent Pt sites to generate NCO surface species. These Pt–NCO species can either react further with adsorbed NOx to form N_2 or they can spillover to Ba and Al sites. An alternative mechanism has also been discussed in the literature, as suggested by Forzatti et al. [23]. The main steps involved in this mechanism are described below:

$$Pt* + CO \rightarrow Pt{-}CO \quad (7)$$

$$-Ba{-}ONO_2 + Pt{-}CO \rightarrow -Ba{-}ONO + CO_2 + Pt* \quad (8)$$

$$-Ba{-}ONO + Pt{-}CO \rightarrow -Ba{-}OCONO + Pt* \quad (9)$$

$$-Ba{-}OCONO + Pt{-}CO \rightarrow -Ba{-}OCNO + CO_2 + Pt* \quad (10)$$

$$-Ba{-}OCNO + Pt{-}CO \rightarrow -Ba{-}NCO + CO_2 + Pt* \quad (11)$$

Reactions (8)–(11) require CO spillover from Pt to Ba sites at the Pt–BaO interface, NOx stored on Ba sites being reduced to NCO in a sequential manner. The intermediates $-CO_2NO$ and –OCNO are assumed to be very reactive (given that they were not detected [23]) and consequently, NOx reduction is likely controlled by the reduction of nitrates to nitrites. According to this scheme, isocyanate formation takes place directly on Ba sites with no NOx release required, while Pt sites act as a conduit for the CO reductant. Our observation of a linear relationship between the increase in Ba–NCO band intensity and the decrease in $Ba–NO_3$ band intensity during catalyst purging with CO suggests that NCO species represent a critical intermediate in LNT regeneration with CO. However, by itself this information does not allow us to distinguish between the foregoing mechanisms for NCO formation.

During rich purging under dry conditions, the formed Ba–NCO (and Al–NCO) species can react with residual nitrate to form N_2 [23,29]:

$$3Ba(NCO)_2 + Ba(NO_3)_2 \rightarrow 4BaO + 4N_2 + 6CO_2 \quad (12)$$

However, the continuous accumulation of Ba–NCO during NOx reduction under dry, rich conditions implies that the reaction is very slow compared to NCO formation. Further reactions of NCO species take place after switching from the rich to the lean phase. Our MS results demonstrate that NCO surface species can be removed by oxidizing gases such as O_2 or NO in the lean phase. Combining the data concerning the evolution of both gas and surface species at 350 °C, the following reactions during the exposure of isocyanate to O_2 are suggested:

$$Ba(NCO)_2 + 3/2O_2 \rightarrow BaO + N_2 + 2CO_2 \quad (13)$$

$$Ba(NCO)_2 + 2O_2 \rightarrow BaO + N_2O + 2CO_2 \quad (14)$$

$$Ba(NCO)_2 + 7/2O_2 \rightarrow BaO + 2NO_2 + 2CO_2 \quad (15)$$

$$Ba(NCO)_2 + 4O_2 \rightarrow Ba(NO_3)_2 + 2CO_2 \quad (16)$$

The simultaneous detection of mass 46 ($^{15}N_2{}^{16}O$) and mass 49 ($^{15}N^{16}O^{18}O$) implies that reactions (14) and (15) occur in parallel, although the reactions are slower than reaction (13). However, the slow evolution of the NCO DRIFTS band, combined with the fast evolution of a relatively small amount of gaseous N-species indicated that most of NCO species are eventually oxidized back to Ba nitrate during the reaction with O_2.

Unlike the reaction with O_2, N_2 seems to be the only product during NCO reaction with NO at 350 °C (Fig. 9), which is very different from TPSR in NO (Fig. 6). At this high temperature, almost no N_2O and NO_2 are released. The evolution of both gaseous and surface species suggests that two main reactions can occur with NO:

$$Ba(NCO)_2 + 3/2NO \rightarrow 2BaO + 3N_2 + 4CO_2 \quad (17)$$

$$Ba(NCO)_2 + 8NO \rightarrow Ba(NO_3)_2 + 4N_2 + 2CO_2 \quad (18)$$

A comparison of N_2 evolution and Ba nitrate formation reveals that there is a delay in the formation of Ba nitrate relative to N_2, which suggests that the kinetics of reaction (18) are slower relative to reaction (17).

Besides the N_2 formation observed during rich purging, N_2 can also be formed in the lean phase, which is consistent with the two N_2 formation peaks reported in the literature (i.e., during the rich phase and immediately after the switch to lean conditions) [28]. A comparison of MS data from isothermal reactions of NCO at 350 °C with O_2 and with NO clearly demonstrated faster kinetics for reaction (13) than reaction (17) at the O_2 and NO concentrations used in this study. Moreover, given that NO/O_2 appeared slightly more reactive than O_2 toward isocyanate in TPSR and ISR experiments, it can be inferred that NO_2 (formed in situ from NO oxidation) is even more active for isocyanate than either O_2 or NO. Hence, it can be concluded that N_2 formation during NOx reduction by CO under dry cycling conditions mainly occurred via isocyanate reaction with $NO + O_2$ after switching to lean conditions.

Both DRIFTS and MS data in this study demonstrated that the reaction between NCO and H_2O is very fast, which is in line with our previous finding that almost no NCO species accumulated on the surface during rich purging with CO when H_2O was present [26]. According to the literature [27], isocyanate species are decomposed through hydrolysis according to the following reaction:

$$Ba(NCO)_2 + 4H_2O \rightarrow Ba(OH)_2 + 2NH_3 + 2CO_2 \quad (19)$$

Unfortunately we were not able to monitor NH_3 in this study due to interference from H_2O, however, the observed delay in N_2 evolution implies that N_2 is not the initial product during NOx reduction. Rather, N_2 formation is suggested to occur through a further reaction between NH_3 and stored NOx:

$$10NH_3 + 3Ba(NO_3)_2 \rightarrow 3Ba(OH)_2 + 8N_2 + 12H_2O \quad (20)$$

NH_3 is a very effective reductant and thus residual nitrate can be reduced by NH_3 formed from hydrolysis of isocyanate species to generate N_2. This finding implies that H_2O plays a crucial role in facilitating NOx reduction with CO. However, under wet cycling conditions with CO as a sole reductant, H_2O can also participate in H_2 generation via the water–gas shift reaction, thereby generating H_2 which functions as a more effective reductant than CO. The relative importance of these two NOx reduction pathways, namely, isocyanate generation followed by hydrolysis and NOx reduction by the resulting NH_3 on the one hand, and NOx reduction by H_2 derived from the WGS reaction on the other, remains to be elucidated. Although recent work by Harold et al. [33] suggests that under steady state conditions NO reduction by CO in the presence of excess water affords NH_3 mainly via the water–gas shift pathway, this may not hold under transient conditions for which storage effects (e.g., of NCO) are typically important. In addition to their reactivity toward NO, O_2 and H_2O, the present study also confirmed that these NCO species can react with nitrate to generate N_2 and CO_2 (as depicted in Eq. (12)). However, both DRIFTS and MS results demonstrated that the kinetics of this reaction are much slower than for both oxidation (O_2 and NO) and hydrolysis of isocyanate, so consumption of isocyanate species through this approach is negligible under cycling conditions.

5. Conclusions

This study investigated the formation of isocyanate during NOx reduction with CO and its reactivity toward different lean exhaust components by means of combined DRIFTS-mass spectrometry measurements. The main findings are summarized as follows:

During NOx reduction by CO under dry lean-rich cycling conditions, significant CO_2 formation occurs immediately after the switch to rich conditions, after which both Pt–CO and NCO bands appear simultaneously. These observations indicate that PtO_x needs to be first reduced to metallic Pt before significant CO adsorption can occur. DRIFTS results verified the formation of both Ba–NCO and Al–NCO species. Ba–NCO formed more rapidly than Al–NCO, and became the dominant isocyanate species on the surface during rich purging. A higher ratio of band intensities was observed between Ba–NCO and Al–NCO at 400 °C relative to 300 °C, suggesting that Ba–NCO is thermally more stable than Al–NCO.

During rich purging at 300 and 400 °C, a near linear relationship was found between the increase in Ba–NCO band intensity and the decrease in Ba–NO_3 band intensity. This suggests that Ba–NCO is directly derived from the reduction of Ba nitrate by CO, i.e., Ba–NCO species represent a critical intermediate in the reduction of stored NOx with CO.

Under dry cycling conditions with CO as the reductant, N_2 is mainly generated via NCO reaction with NO + O_2 after the switch to lean phase conditions, rather than being formed during the rich phase. However, the evolution of DRIFT spectra under both temperature-programmed and isothermal reaction modes revealed that H_2O is the most reactive species with respect to isocyanate of those tested (H_2O, O_2, NO, NO/O_2). Simultaneous monitoring of surface and gaseous species inferred that N_2 is not the first product of the reaction of isocyanate with H_2O. Instead, N_2 originated from a secondary reaction of NH_3 with residual nitrate.

Disclaimer

Acknowledgements

This project was funded by the U.S. Department of Energy (DOE) under award number DE-EE0000205. Oak Ridge National Laboratory is managed by UT-Battelle, LLC, for the U.S. Department of Energy under contract number DE-AC05-00OR22725.

References

[1] E. Fridell, M. Skoglundh, B. Westerberg, S. Johansson, G. Smedler, Journal of Catalysis 183 (1999) 196.
[2] N.W. Cant, M.J. Patterson, Catalysis Today 73 (2002) 271.
[3] W.S. Epling, L.E. Campbell, A. Yezerets, N.W. Currier, J.E.II. Parks, Catalysis Reviews 46 (2004) 163.
[4] L. Castoldi, I. Nova, L. Lietti, L.P. Forzatti, Catalysis Today 96 (2004) 43.
[5] I. Nova, L. Lietti, I. Castoldi, E. Tronconi, P. Forzatti, Journal of Catalysis 239 (2006) 244.
[6] L. Lietti, I. Nova, P. Forzatti, Journal of Catalysis 257 (2008) 270.
[7] W.P. Partridge, J.S. Choi, Applied Catalysis B 91 (2009) 144.
[8] R.D. Clayton, M.P. Harold, V. Balakotaiah, Applied Catalysis B 84 (2008) 616.
[9] L. Cumaranatunge, S.S. Mulla, A. Yezerets, N.W. Currier, W.N. Delgass, F.H. Ribeiro, Journal of Catalysis 246 (2007) 29.
[10] I. Nova, L. Lietti, P. Forzatti, Catalysis Today 136 (2008) 128.
[11] Y. Ji, J.-S. Choi, T.J. Toops, M. Crocker, M. Naseri, Catalysis Today 136 (2008) 146.
[12] Y. Ji, C. Fisk, V. Easterling, U. Graham, A. Poole, M. Crocker, J.-S. Choi, W. Partridge, K. Wilson, Catalysis Today 151 (2010) 362.
[13] N. Takahashi, K. Yamazaki, H. Sobukawa, H. Shinjoh, Applied Catalysis B 70 (2007) 198.
[14] D. James, E. Fourre, M. Ishii, M. Bowker, Applied Catalysis B 45 (2003) 147.
[15] J.P. Breen, C. Rioche, R. Burch, C. Hardacre, F.C. Meunier, Applied Catalysis B 72 (2007) 178.
[16] T. Szailer, J.H. Kwak, D.H. Kim, J.C. Hanson, C.H.F. Peden, J. Szanyi, Journal of Catalysis 239 (2006) 51.
[17] Z.Q. Liu, J.A. Anderson, Journal of Catalysis 224 (2004) 18.
[18] H. Abdulhamid, E. Fridell, M. Skoglundh, Applied Catalysis B 62 (2006) 319.
[19] N.W. Cant, M.J. Patterson, Catalysis Letters 85 (2003) 153.
[20] C.M. Scholz, B.H. Maes, M.H. de Croon, J.C. Schouten, Applied Catalysis A 332 (2007) 1.
[21] M. Al-Harbi, W.S. Epling, Applied Catalysis B 89 (2009) 315.
[22] I. Nova, L. Lietti, P. Forzatti, F. Frola, F. Prinetto, G. Ghiotti, Topics in Catalysis 52 (2009) 1757.
[23] P. Forzatti, L. Lietti, I. Nova, S. Morandi, F. Prinetto, G. Ghiotti, Journal of Catalysis 274 (2010) 163.
[24] S. Morandi, G. Ghiotti, L. Castoldi, L. Lietti, I. Nova, P. Forzatti, Catalysis Today 176 (2011) 399.
[25] L. Castoldi, L. Lietti, R. Bonzi, N. Artioli, P. Forzatti, Journal of Physical Chemistry C 115 (2011) 1277.
[26] Y. Ji, T. Toops, J. Phil, M. Crocker, Applied Catalysis B 91 (2009) 329.
[27] T. Lesage, C. Verrier, P. Bazin, J. Saussey, M. Daturi, Physical Chemistry Chemical Physics 5 (2003) 4435.
[28] J.P. Breen, R. Burch, C. Fontaine-Gautrelet, C. Hardacre, C. Rioche, Applied Catalysis 81 (2008) 150.
[29] C.D. DiGiulio, V.G. Komvokis, M.D. Amiridis, Catalysis Today 184 (2012) 8.
[30] Y. Ji, T.J. Toops, M. Crocker, Catalysis Letters 119 (2007) 257.
[31] N. Bion, J. Saussey, M. Haneda, M. Daturi, Journal of Catalysis 217 (2003) 47.
[32] B.A. Morrow, L.E. Moran, Journal of Physical Chemistry 81 (1977) 2667.
[33] P.R. Dasari, R. Muncrief, M.P. Harold, Catalysis Today 184 (2012) 43.